



Structure and energetics of the anisole-Arn (n=1, 2, 3) complexes: high-resolution resonant two-photon and threshold ionization experiments, and quantum chemical calculations

Journal:	<i>Physical Chemistry Chemical Physics</i>
Manuscript ID:	CP-ART-02-2015-001166.R1
Article Type:	Paper
Date Submitted by the Author:	31-Mar-2015
Complete List of Authors:	Mazzoni, Federico; Università di Firenze, Dipartimento di Chimica 'Ugo Schiff' and LENS Becucci, Maurizio; Università di Firenze, Dipartimento di Chimica 'Ugo Schiff' and LENS Řezáč, Jan; Institute of Organic Chemistry and Biochemistry, Academy of Sciences of the Czech Republic, Nachtigalová, Dana; Institute of Organic Chemistry and Biochemistry, Academy of Sciences of the Czech Republic, Michels, Francois; University of Manchester, Photon Science Institute and School of Chemistry Hobza, Pavel; Academy of Sciences of the Czech Republic, Institute of Organic Chemistry and Biochemistry Muller-Dethlefs, Klaus; University of Manchester, Photon Science Institute and School of Chemistry

Structure and energetics of the anisole-Ar_n (n=1, 2, 3) complexes: high-resolution resonant two-photon and threshold ionization experiments, and quantum chemical calculations

Federico Mazzoni^{ab}, Maurizio Becucci^a, Jan Řezáč^c, Dana Nachtigallová^c, François Michels^b, Pavel Hobza^{*cd} and Klaus Müller-Dethlefs^b

^aDipartimento di Chimica 'Ugo Schiff' Università di Firenze, via della Lastruccia 3 and LENS, via N. Carrara 1, 50019 Sesto Fiorentino (FI), Italy

^bPhoton Science Institute and School of Chemistry, The University of Manchester, Oxford Road, Manchester M13 9PL, United Kingdom

^cInstitute of Organic Chemistry and Biochemistry, Academy of Sciences of the Czech Republic, Flemingovo nám. 2, 166 10 Prague 6, Czech Republic

^dRegional Centre of Advanced Technologies and Materials, Department of Physical Chemistry, Palacký University, 771 46 Olomouc, Czech Republic

We present a concerted experimental and theoretical study of the anisole...Ar_n complexes with n=1-3. Experimentally, anisole was seeded into a pulsed supersonic argon jet producing a molecular beam. Resonant two-photon, two-colour ionisation (R2PI) spectra of anisole...Ar_n complexes with n=1-3 were obtained. Also, the photodissociation of the (1:1) cluster was probed synchronously by - *Zero Electron Kinetic Energy Photoelectron Spectroscopy* (ZEKE) - and - *Mass Resolved Threshold Ionization* (MATI) - measuring electrons and ions obtained from pulsed field ionization of high-*n* Rydberg states upon two-colour laser excitation. The experimental results are compared to quantum chemical calculations at the DFT-D3 (B-LYP/def2-QZVP level with Grimme's D3 dispersion correction) level. Structure and energetics due to microsolvation effects by the direct interaction of the argon atoms with the π -system were evaluated. The experimental binding energy of the 1:1 cluster is finally compared to computational results; in the *S*₀ ground state the theoretical value based on the "gold standard" CCSD(T)/CBS calculations lies within the error bars of the observed value. In the excited state the agreement between theory and experiment is not so spectacular but relative

values of observed dissociation energies (D_0) in the ground and excited states and of calculated ones agree well.

Introduction

The study of molecular clusters formed by an aromatic molecule and a rare gas atom in supersonic jet expansions —molecular beams— have provided many insights on the nature and strength of intermolecular forces and non-covalent interactions. For many systems, a comparison to highest level quantum calculations has been possible and, for example, complexes with benzene, aniline, phenol and other analogue molecules with argon are probably the most studied.¹⁻¹¹

Typically, the first argon atom interacts directly with the aromatic electron system. The interaction energy is around 400 to 500 cm^{-1} in the neutral S_0 ground state and the distance between the argon atom and the aromatic plane is about 3.5 Å. The first allowed singlet electronic transition in the cluster is normally red shifted ($\sim 30\text{-}40 \text{ cm}^{-1}$) with respect to that of the corresponding chromophore molecule. It indicates an increase of the interaction in the excited states, where the polarization of the aromatic system is larger.

The second argon atom is usually on the opposite side of the aromatic ring, directly interacting with the π -system and causing a doubling of the band shift for the origin of the spectrum. This is the case, for example, for phenol and aniline complexes.⁵⁻⁷ Less stable conformers have also been observed with the second argon atom on the same side of the ring, resulting in small blue shifts (aniline)⁷ or in negligible shifts (phenol)⁸ with respect to the bare molecule.

Also clusters with three argons show two possible configurations. The most stable is usually with the three argon atoms on the same side of the ring and the relative band is blue-shifted with respect to the bare molecule. The second possible configuration is to have two argon

atoms on the same side of the ring and the third on the opposite side, and its signature in the spectrum is usually red shifted with respect to the bare molecule.⁵⁻⁸

The standard experimental approach for the study of these systems is the production of the clusters in a molecular beam by seeding a molecule into an adiabatic supersonic jet expansion of a noble gas (He, Ne, Ar) suitable gas mixture and their probing with laser spectroscopic methods. The most used is the resonance enhanced two-photon ionization (R2PI) scheme, coupled with ion time of flight (TOF) mass analysis and detection. A dramatic breakthrough in the energy resolved spectroscopic studies on the ionic particles was represented by the high-resolution threshold ionization experiments of Pulsed Field Ionization of high- n Rydberg states. This is normally done by detection of either electrons (ZEKE) or ions (MATI).¹⁻³ At the same time, structural properties and large amplitude motions in these systems were probed by rotationally resolved spectroscopic methods in the ground state (microwave absorption) and/or electronic excited states (high resolution laser induced fluorescence).^{9,10}

Earlier investigations of complexes of aromatic molecules with rare gas atoms showed that the stabilization energy in these complexes is rather small (about 1 kcal/mol) and stems almost exclusively from the dispersion energy. This means that it is imperative, for computational procedures, to use most accurate quantum mechanical (QM) methods covering a large portion of correlation energy. Structure, stabilization energy and vibration frequencies of benzene...rare gas complexes were investigated at MP2, MP4 and CCSD(T) levels and theoretical characteristics were shown to be in a reasonable agreement with the respective experimental values.^{12,13} For larger benzene...Ar_n (n=2-8) clusters attention was not only focussed on the stabilization energies but also on populations of single clusters.¹⁴ A significant population of the energetically less favourable one-sided structure of the benzene...Ar₂ complex was explained by the entropy effect.¹⁵ Using MD simulations also the nuclear

structure of the dynamics of benzene...Ar_n was investigated.¹⁶ Structure and stabilization energy of different conformers of the phenol...Ar complex was thoroughly investigated and the theoretical D₀ energy, constructed as a sum of the CCSD(T)/CBS interaction energy and the difference of the zero-point vibration energy, agreed fairly well (within about 30 cm⁻¹) with the respective experimental value obtained from ZEKE/MATI measurements.¹⁷ Analyzing possible sources of error it was shown that ΔZPVE energies were determined with lower accuracy than the interaction energy and for possible improvements inclusion of anharmonicity is required.

Contrary to benzene, anisole is known to form clusters with different molecules through interaction with the aromatic electron density¹⁸ or with the lone pair of electrons on the oxygen atom^{19,20} or even with other secondary in-plane interactions.^{21,22}

Here we present a R2PI study on the anisole-argon clusters containing from 1 to 3 argon atoms (from now on labelled as (1:n) clusters, n=1,..,3) and a ZEKE/MATI study of the 1:1 cluster. The solvation effects of the argon atoms to the electronic functions of the anisole have been evaluated theoretically using the DFT-D method. The equilibrium geometries of the different clusters were calculated at the same theoretical level. Moreover, we present the first application of the new method^{2,23} for the synchronous acquisition of ZEKE and MATI spectra to the anisole...argon 1:1. The binding energy so obtained is compared to theoretical values based on CCSD(T)/CBS (ground state) and ADC(2) calculations (electronically excited state), respectively.

Methods

Experimental

R2PI and MATI-ZEKE experiments have been carried on using the same apparatus described in previous reports.^{24,25} Briefly, a supersonic molecular beam is formed, using Argon as carrier gas, by means of a pulsed valve General Valve Series 9, with a 0.5mm nozzle. The central and coldest part of the expansion, for which the concentration of clusters is highest, is selected by a 1.5 mm diameter skimmer placed at about a distance of 4 cm from the nozzle. The resulting molecular beam is crossed perpendicularly by two co-propagating laser beams in a pump and probe experimental configuration. The excitation region is located between the electrodes of a capacitor, acting as an electrostatic lens for charged particles. The UV pulsed radiation is obtained by the frequency doubled emission of two dye lasers synchronously pumped by a Nd:YAG laser.

For the R2PI experiment, a high positive voltage of *ca.* 800V is applied to the upper electrode plate of the extraction system after the laser excitation, in order to push the ions downwards into the reflectron time of flight (RETOF) spectrometer, the ions are then detected by a MCP detector.

ZEKE-MATI experiments were synchronously performed using a new setup that was developed specifically for the study of van der Waals clusters photodissociation.²³ The low voltage pulse sequence employed for the synchronous ZEKE-MATI experiment is reported in Fig. 1, and a brief description of this sequence is reported hereafter. About 300 ns after the laser excitation a small positive voltage (1.2 V) is applied to lower extraction plate in order to separate directly ionized particles from neutral Rydberg particles (called Rydbergs from now on) that still fly in the same direction of the beam: the charged particles move to the upper, grounded, extraction plate. Then, after 17 μ s, a negative, very short pulse (-2.4 V, 200 ns) is applied to the same lower extraction plate, in order to field ionize the Rydberg states. Zero Kinetic Energy electrons are produced and pushed upwards over the upper grid, where they

are post accelerated (a 10 V accurately synchronized pulse is used) into a linear time of flight drift tube and collected by an MCP. Directly produced ions and both ionized and neutral Rydbergs still fly for about 3 μs . Then, *ca.* 20 μs after the laser excitation, a high voltage positive pulse is applied to the upper extraction plate: Rydbergs, that are still neutral, are field ionized and pushed downwards into the RETOF. In the resulting mass spectrum two peaks will hence appear for every species: the first one from to direct/spontaneous ionization, and the latter, from field ionized Rydbergs.

In the experiments, four mass channels have been monitored to probe the dissociation process of the anisole \cdots Ar complex: two of them for the anisole \cdots Ar parent ions (R2PI and MATI signals) and the other two for the ionic anisole fragment (again, R2PI and MATI signals).

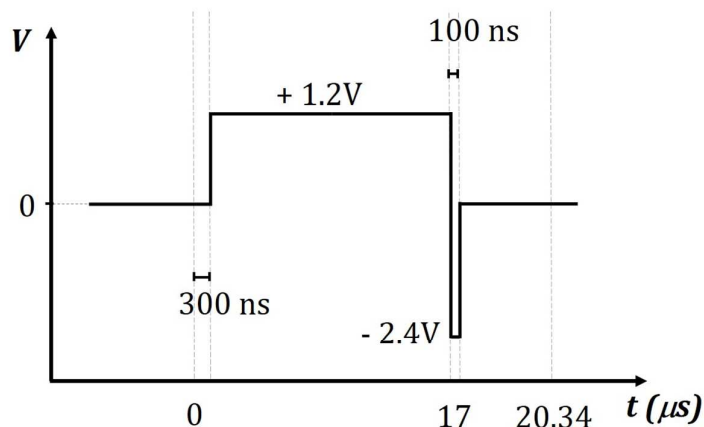


Fig. 1. Low voltage pulse sequence for the synchronous MATI-ZEKE experiment with a schematic view of the laser excitation and the final position of the charged particles (up) and the neutral particles (still in the beam). The zero time of the experiment is set at the laser pulse arrival time.

Computational

Geometry optimizations, scans of the intermolecular potentials and vibrational analysis were carried out at B-LYP/def2-QZVP level with Grimme's D3 dispersion correction (we refer to

this setup as to DFT-D3 in the rest of the paper).^{26,27} This combination of functional and large def2-QZVP basis set,²⁸ along with the use of the Becke-Johnson damping function in the dispersion correction²⁹⁻³¹ had been shown to yield very accurate interaction energies.³² The DFT calculations were performed in Turbomole package³³ using the resolution of identity approximation.

Interaction energies in the stationary points were calculated using the composite CCSD(T)/CBS approach³⁴ with counterpoise correction for basis set superposition error.³⁵ The CCSD(T)/CBS energies were obtained by combining HF/aug-cc-pVQZ energy, MP2 correlation energy extrapolated³⁶ from aug-cc-pVTZ and aug-cc-pVQZ basis sets³⁷ and the CCSD(T) correction (defined as $E^{\text{CCSD(T)}} - E^{\text{MP2}}$) calculated in the aug-cc-pVDZ basis set.

The excited state calculations were performed using the second-order algebraic diagrammatic construction ADC(2)³⁸⁻⁴⁰ method which is related to the CIS(D) or CC2 methods. The ADC(2) can be seen as "MP2 for the excited states" and, thus, it covers the dominant part of the correlation energy.^{28,41,42} As shown in several recent studies many body electron correlations effects are important to obtain reliable results of excitation energies.^{43,44} The calculations were performed with the resolution-of-identity approach and def2-TZVP basis set.^{28,41}

Experimental results

The R2PI spectra of the anisole...Ar_n (n = 1, 2, 3) complexes were recorded for excitation energies between 36230 and 36430 cm⁻¹. In Fig. 2 the electronic spectra of the different complexes are compared to the origin band of the anisole electronic spectrum. For each spectrum we assign the strongest peak at lower frequency as the origin band, as was done for similar clusters.⁴⁵ It is immediately evident that the origin bands in the electronic spectra of the complexes are red shifted with respect to the origin band of the anisole spectrum. The relative shifts are reported in Table 1. It is important to note that the band shift for the origin

of the (1:2) complex spectrum is twice that of the (1:1) complex, while the shift for the (1:3) complex is almost the same as for the (1:2). As the spectra of the (1:2) and (1:3) clusters are very similar, we show their details in Fig. 3. The existing differences demonstrate that these two spectra are independent and not contaminated from dissociation of larger clusters.

	$S_1 \leftarrow S_0$ (cm ⁻¹)	Shift (cm ⁻¹)
anisole	36384	-
(1:1)	36346	-38
(1:2)	36307	-77
(1:3)	36308	-76

Table 1 Origin band shifts for R2PI spectra of the complexes. The shifts are calculated with respect to the bare anisole origin band

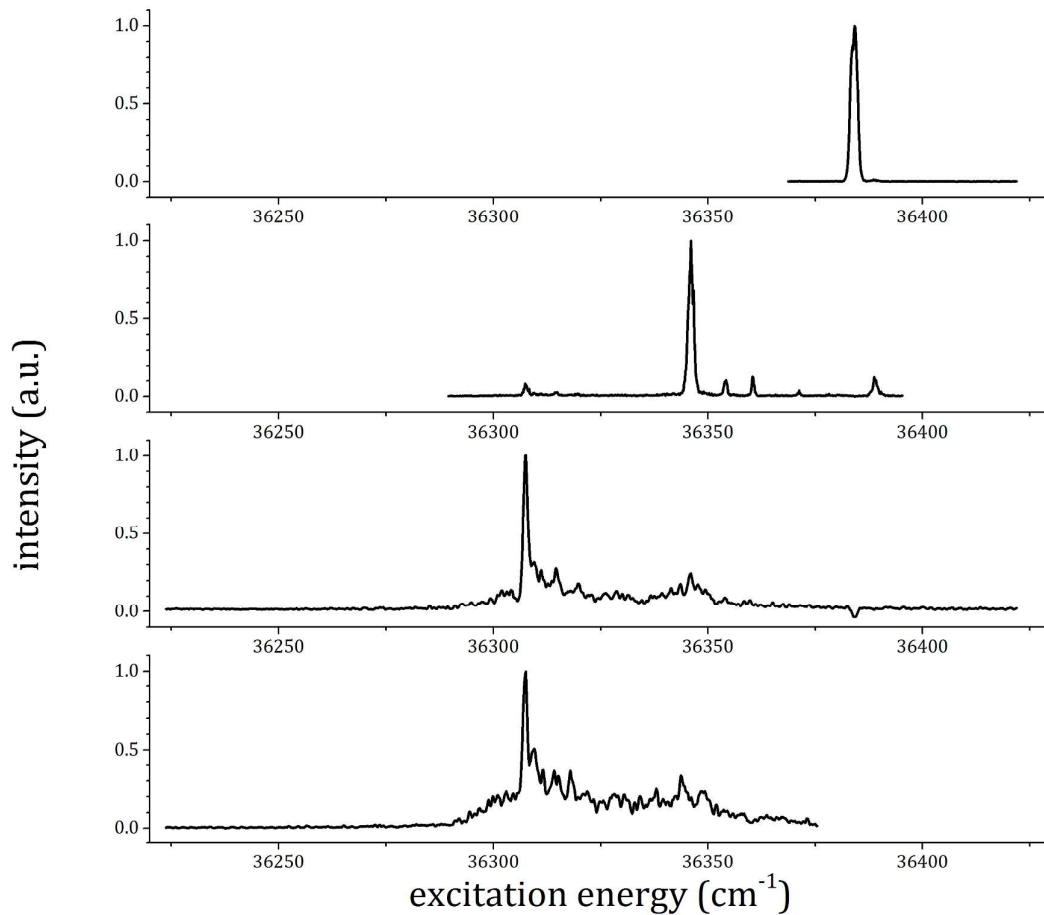


Fig. 2. Comparison between the observed R2PI spectra of anisole...Ar_n complexes. The origin band of R2PI spectrum of anisole is also reported. The probe laser is set to 31250 cm⁻¹. Starting from the top, the spectra refer respectively to anisole, (1:1), (1:2) and (1:3) complexes.

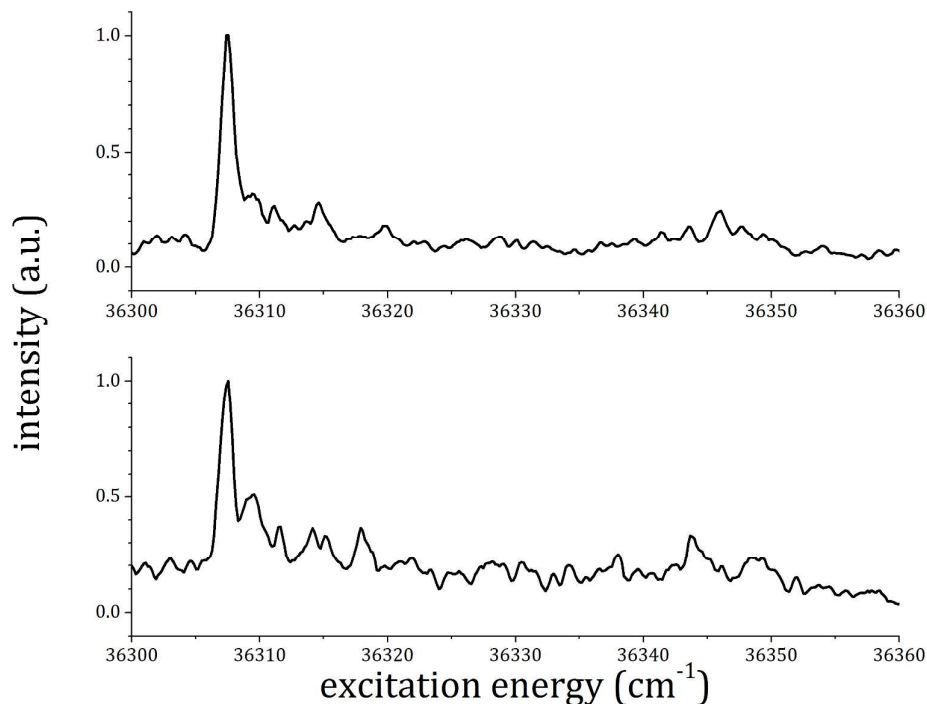


Fig. 3. Detail of the R2PI spectra of the (1:2) (top) and (1:3) (bottom) clusters in the origin band spectral region. Different features are present in the two spectra, showing that both spectra are not contaminated by the fragmentation of larger clusters.

The (1:1) cluster was then studied in details with the synchronous ZEKE-MATI experiment. ZEKE, PIE and MATI spectra have been recorded between 66100 and 66900 cm⁻¹ with the first laser held in resonance with the origin band of the (1:1) cluster at 36386 cm⁻¹. The same experiment has been carried out with the pump laser in resonance with the first and the second vibronic bands. Among these data-sets, the only one showing a significant signal is the highly sensitive ZEKE with excitation through the first vibronic band, so we will not present the others. Fig. 4 shows the ZEKE spectra measured when the pump laser is held in resonance with the origin band and with the first vibronic transition of the R2PI spectrum. In the first spectrum two different band sets are evident, one starting at 66203 cm⁻¹ and the second one at 66784 cm⁻¹. In the second spectrum the only transition observed is the one at 66203 cm⁻¹.

That excitation energy is therefore assigned to the ionization potential (IP) of the complex. Table 2 reports all the observed transitions when the excitation occurs through the origin band of the electronic spectrum. The resulting red shift with respect to the monomer IP (66399 cm^{-1})⁴⁶ is 196 cm^{-1} .

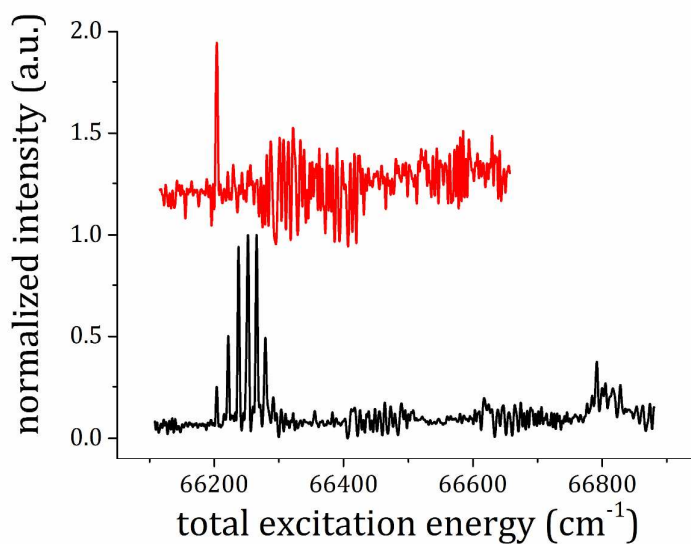


Fig. 4. ZEKE spectra of the anisole...Ar complex. The pump laser is in resonance with the origin band of the R2PI spectrum at 36346 cm^{-1} (lower trace) and with the first vibronic transition at 36354 cm^{-1} (upper trace). The first accessible transition, corresponding to the IP of the cluster, is at 66203 cm^{-1} .

Total excitation energy (cm ⁻¹)	Frequency Shift (cm ⁻¹)		Total excitation energy (cm ⁻¹)	Frequency Shift (cm ⁻¹)
66203	0 <i>origin band</i>		66784	581 <i>internal vibration</i>
66222	19		66791	588 (581+7)
66238	35		66800	597 (581+16)
66253	50		66805	602 (581+21)
66266	63		66816	613 (581+32)
66279	76		66828	625 (581+46)
66292	89		-	-

Table 2 Observed transitions in the ZEKE spectrum with pump laser in resonance with the origin band of the R2PI spectrum

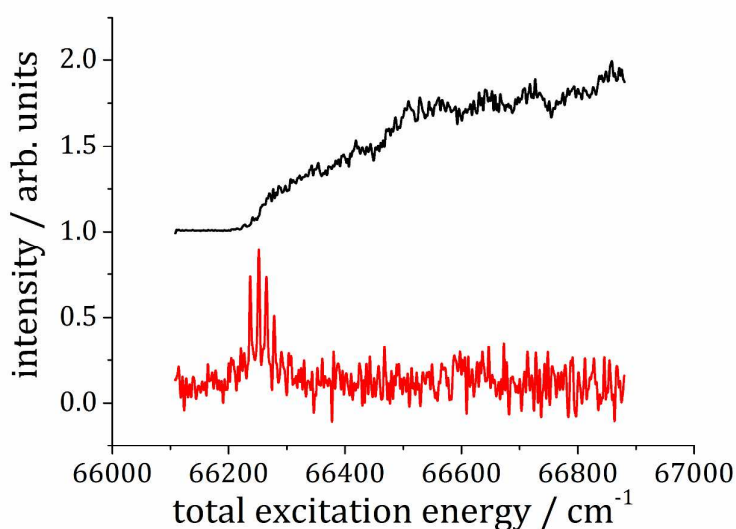


Fig. 5. PIE (upper trace) and MATI (lower trace) spectra recorded at the mass channel of the (1:1) cluster

In Fig. 5 the MATI and PIE spectra for the parent mass channel are reported. Comparing the MATI spectrum with the ZEKE one, the first set of transitions is easily recognised while the second band set is not present. As usual, the signal to noise ratio is much higher in ZEKE than in MATI experiments.

In Fig. 6 the traces of PIE and MATI spectra for the daughter mass channel are presented. In the PIE spectrum the signal starts rising above 66800 cm^{-1} , clearly indicating the spectral region where dissociation occurs. It is important to note that the second band set in the ZEKE spectrum occurs in the same spectral region where the dissociation occurs. Probably, it is quite difficult to see the MATI signal in the fragment channel due to the low signal-to-noise ratio and to the relative weakness of this band set with respect to the first one. Anyway, by the comparison of fragment PIE and ZEKE, the band at 66784 cm^{-1} in the ZEKE spectrum can be taken as the upper limit for the dissociation energy of the complex, being the lowest optically accessible state in the region where dissociation occurs. This determination leads to a value of $581 \pm 5\text{ cm}^{-1}$ for the binding energy in the ionic ground state, and consequently $423 \pm 5\text{ cm}^{-1}$ in the neutral first excited state and $385 \pm 5\text{ cm}^{-1}$ in the neutral ground state, as indicated by the correlation diagram reported in Fig. 7.

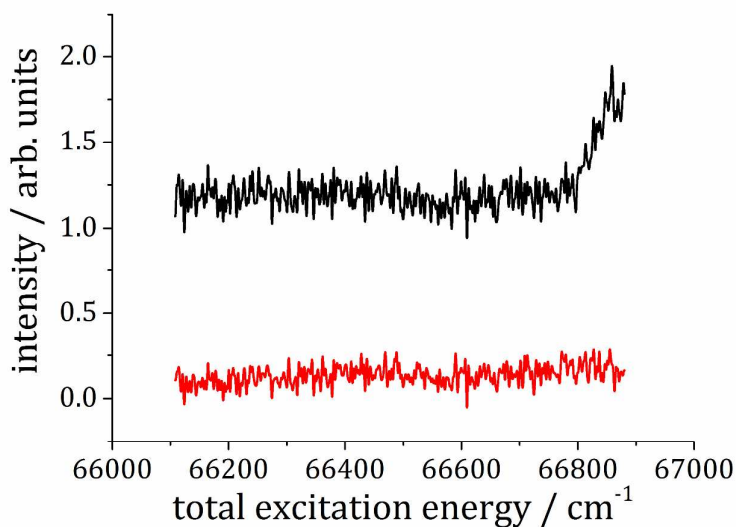


Fig. 6. PIE (upper trace) and MATI (lower trace) spectra recorded at the mass channel of the anisole fragment. It is clearly evident that a dissociation occurs above 66800 cm^{-1} . Almost no evidence for a clear dissociation threshold in the MATI spectrum is present, probably because of the low signal-to-noise ratio.

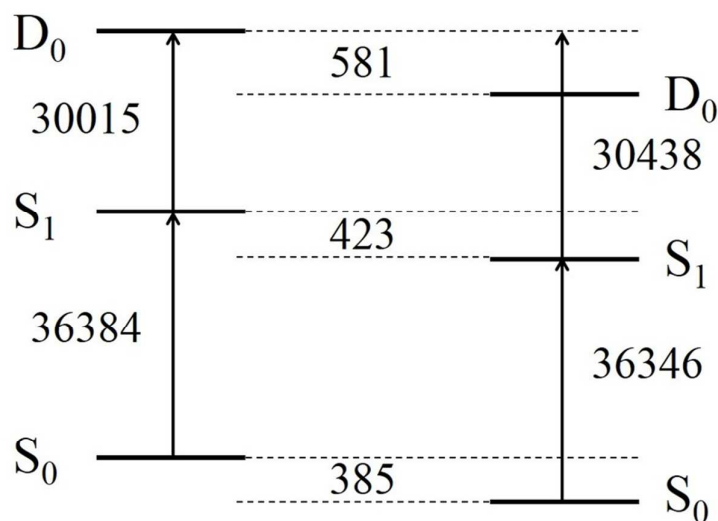


Fig. 7. Correlation diagram for the electronic states of anisole monomer (left) and anisole...Ar 1:1 complex (right). In the middle the experimentally determined upper limits for the binding energies in the different relevant states are reported.

Computational Results

Geometry of the complexes. The geometries of the complex of anisole with one and two argon atoms are well defined and can be easily optimized. Energetically most favourable binding mode is the interaction of the argon atom with the aromatic ring of the anisole; in the (1:2) complex, the two atoms are placed symmetrically on the opposite side of the ring plane (see Fig. 8). The third argon atom lies in the plane of the ring. To obtain all the possible positions it can occupy, we performed a scan of the potential energy surface at the DFT-D3 levels. The six minima obtained from the scan were further optimized using DFT-D3 and the final interaction energies were calculated at the CCSD(T)/CBS level. The positions of the minima along with their CCSD(T)/CBS interaction energies are shown in the potential energy surface plotted in Fig. 9. The minima are energetically very close and the barriers separating

them are low. However, the vibrational temperature of the clusters in the molecular beam is very low (estimated to be 6 ± 2 K) what makes the transitions between the minima unlikely.

The most important geometric characteristics of the complexes is the distance between the plane of the aromatic ring and the argon atoms. In the (1:1) complex it amounts to 3.524 Å. No significant change can be detected when the other argon is added at the opposite side and when the third one is added.

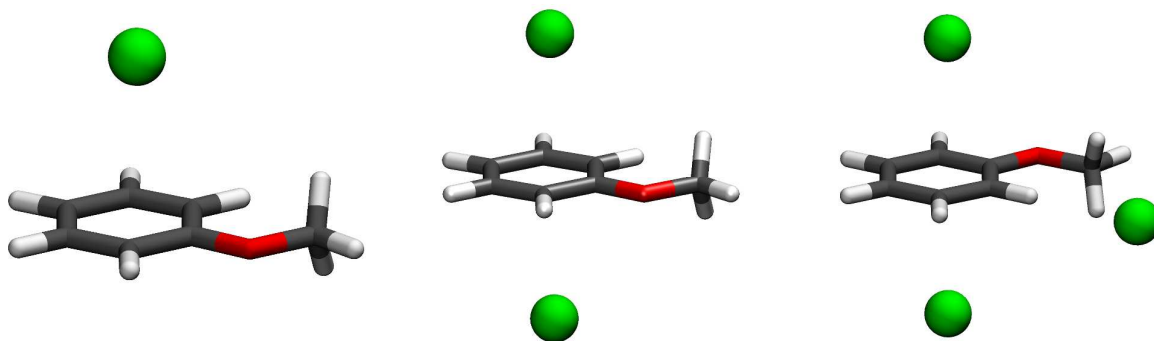


Fig. 8. Optimized geometries of the complexes of anisole with one, two and three argon atoms. In the latter, only the global minimum is shown but other minima with the third argon atom at various positions in the plane are very close in energy.

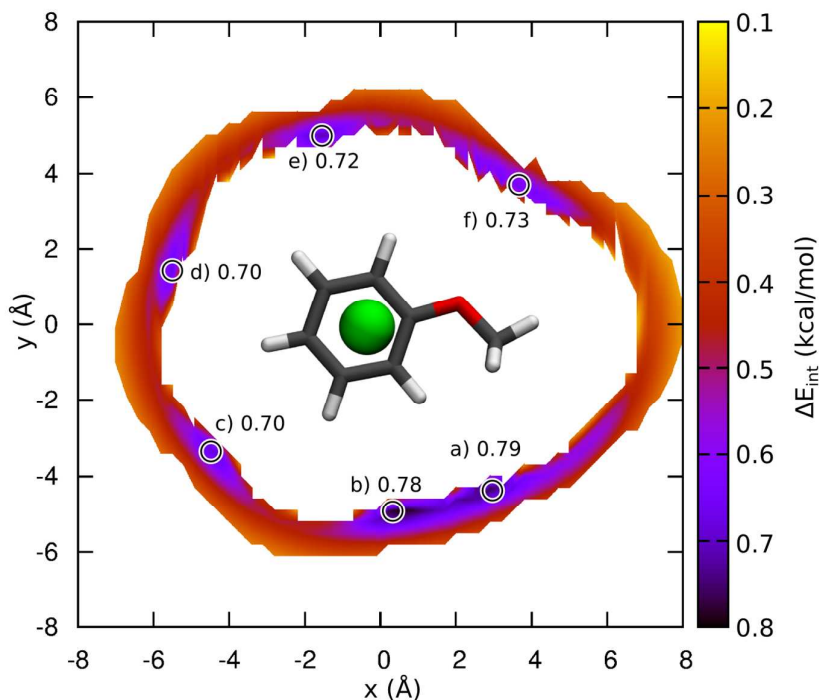


Fig. 9. Potential energy (kcal/mol, calculated at DFT-D3 level, scale shifted to match the CCSD(T)/CBS results) of the third Ar atom added to the (1:2) complex. The six minima, labelled a) to f), were optimized and their CCSD(T)/CBS interaction energies are provided in the plot.

Anisole...Ar dissociation energy. For both the neutral and positively charged (1:1) complex the dissociation energy was calculated as a sum of the interaction energy ΔE , change of zero point vibrational energy $\Delta ZPVE$ and deformation energy E^{def} (the dissociation energy is defined as positive). Table 3 lists the individual components as well as the final D_0 based on the CCSD(T)/CBS interaction energy. The D_0 in the neutral complex is 1.11 kcal/mol (389 cm^{-1}), in the cationic complex it amounts to 1.73 kcal/mol (605 cm^{-1}).

To test the validity of the harmonic approximation used in the calculation of $\Delta ZPVE$, we have calculated the anharmonicity of the intermolecular stretching mode, which contributes to the $\Delta ZPVE$ with 25 cm^{-1} . At the DFT-D3 level, we performed a scan along the normal mode and fitted it with Morse potential for which the vibrational energy levels can be expressed

analytically. However, the anharmonic zero point energy in this mode differs from the harmonic one only marginally, by -0.4 cm^{-1} .

component	method	neutral	cation
ΔE	CCSD(T)/CBS	1.31	1.76
	DFT-D3	1.19	1.84
$\Delta ZPVE$	DFT-D3	-0.19	-0.02
E^{def}	DFT-D3	-0.004	-0.01
D_0	composite	1.11	1.73

Table 3 Components of the dissociation energy and the final D_0 (in kcal/mol) in neutral and cation-radical anisole-argon 1:1 complex. The composite value is sum of CCSD(T)/CBS interaction energy and DFT-D3 $\Delta ZPVE$ and E^{def} .

Excited states of anisole...Ar(n) complexes. The results of the calculations of the vertical energies of the lowest excited states of anisole...Ar(n) complexes are shown in Table 4. For all complexes, the wavefunction of the first excited state is characterized mainly by HOMO (π) \rightarrow LUMO (π^*) electronic configuration. The interaction of Ar atoms with π system of anisole decreased the excitation energies by 40 and 43 cm^{-1} when placed from one or both sides of the aromatic ring, respectively. Only negligible shift in the excitation energy was observed when Ar atom was placed in the plane of the anisole ring. The interaction energy (with corrections for BSSE) of Ar and anisole in the first excited state of anisole...Ar complex was calculated using the ADC(2)³⁸⁻⁴⁰ method as -1.211 kcal/mol . Thus, the interaction energy is about 15% larger than that of the ground stated (-1.053 kcal/mol) interaction energy calculated at the same level.

n	ΔE_{exc}	ΔE_{shift}
0	39600	
1	39560	-40
2	39517	-83
3	39514	-86

Table 4 The vertical excitation energies (in cm^{-1}) in anisole...Ar_n complexes. ΔE_{shift} is the difference in excitation energies with respect to anisole

Further discussion

The most stable calculated geometries of 1:1 and 1:2 clusters of anisole...Ar_n look almost the same as those of the corresponding aniline and phenol clusters. However, the 1:3 cluster geometry shows a very peculiar feature: the most stable structure has the first two argon atoms on opposite sides of the aromatic ring while the position of the third argon is in the plane, where different minima of comparable energy exist. It is therefore possible that more than one isomer is formed and even that the third argon atom is allowed to move from one position to the other.

The microsolvation effects due to the presence of a direct interaction between the argon atom and the π -system are the same as in the case of the simplest reference systems (again, phenol and aniline) and are accurately reproduced by the quantum calculations at the used level of theory. The direct interaction results in a red shift of the electronic functions of about 40 cm^{-1} and their effect is additive when the argon atom lie on opposite sides of the ring. In this case we can observe that the effect of the in-plane argon atom is instead negligible, as the interaction is not with the π -system, but with the σ orbitals of the hydrogen atoms on the ring.

As the differences of the (1:1) complex structure and energetics with respect to the reference systems are negligible,^{2,4} the binding energies are extremely similar, being $385 \pm 5 \text{ cm}^{-1}$ in the

neutral ground state ($364 \pm 13 \text{ cm}^{-1}$ for phenol...Ar and $380 \pm 15 \text{ cm}^{-1}$ for aniline) and $581 \pm 5 \text{ cm}^{-1}$ in the ionic state ($535 \pm 3 \text{ cm}^{-1}$ for phenol...Ar and $495 \pm 15 \text{ cm}^{-1}$ for aniline). Experimental values agree well with the calculated results, in particular for the D_0 energy in the neutral ground state. In addition, good agreement was found for relative values of experimentally obtained D_0 energies in the ground and excited states and those of calculated interaction energies in the ground and excited states.

Conclusion

The structure and the energetic properties of the Anisole...Ar_n (n=1, 2, 3) complexes have been studied in the neutral and first excited state both experimentally and theoretically. R2PI spectroscopy and DFT-D calculations reveal that the contribution of the Ar atom to the electronic functions of the anisole ring is additive for n=1 and n=2, when the Ar is positioned over the ring and is negligible for n=3 when the third Ar atom is lying somewhere else on a PES without clear absolute minima.

For the (1:1) complex the ionization energy (IE) and the binding energy (BE) have been determined, with an improved ZEKE, MATI and PIE experiment. The observed BE is relatively smaller (about 30 cm^{-1}) with respect to the observed one for the phenol...Ar. Calculated BE for the ground state of anisol...Ar lies within the error bars of the observed value. In the excited state the agreement between theory and experiment is not so spectacular but relative values of observed D_0 energies in the ground and excited states and of calculated ones agree well.

Further studies will be necessary for the BEs and the IPs of the (1:2) and (1:3) complexes.

Acknowledgements

This work was part of the Research Project RVO: 61388963 of the Institute of Organic Chemistry and Biochemistry, Academy of Sciences of the Czech Republic. This work was also supported by the Czech Science Foundation [P208/12/G016] and the operational program Research and Development for Innovations of the European Social Fund (CZ 1.05/2.1.00/03/0058). Financial support was coming also from the Italian MIUR and the EU under contract number RII3-CT-2003-506350. F.M. acknowledges financial support from Regione Toscana (Italy).

References

- ¹ H. J. Neusser, H. Krause, *Chem. Rev.*, 1994, **94**, 1829.
- ² C. E. H. Dessent, S. R. Haines, and K. Müller-Dethlefs, *Chem. Phys. Lett.*, 1999, **315**, 103.
- ³ X. Tong, A. Armentano, M. Riese, M. BenYezzar, S.M. Pimblott, K. Müller-Dethlefs, S. Ishiuchi, M. Sakai, A. Takeda, M. Fujii and O. Dopfer, *J. Chem. Phys.*, 2010, **133**, 154308.
- ⁴ Q. Gu, J.L. Knee, *J. Chem. Phys.*, 2008, **128**, 064311.
- ⁵ A. Armentano, J. Černý, M. Riese, M. Taherkhani, M. Ben Yezzar and K. Müller-Dethlefs, *Phys. Chem. Chem. Phys.*, 2011, **13**, 6077.
- ⁶ S. R. Haines, C. E. Dessent and K. Müller-Dethlefs, *Journal of Electron Spectroscopy and Related Phenomena*, 2000, **108**, 1.
- ⁷ P. Hermine, P. Parneix, B. Coutant, F.G. Amar, and Ph. Bréchnignac, *Z. Phys. D -Atoms, Molecules and Clusters*, 1992, **22**, 529.

- ⁸ S-i. Ishiuchi, M. Miyazaki, M. Sakai, M. Fujii, M. Schmies and O. Dopfer, *Phys. Chem. Chem. Phys.*, 2011, **13**, 2409.
- ⁹ M Becucci, G Pietraperzia, NM Lakin, E Castellucci, and P Bréchnac, *Chem. Phys. Lett.*, 1996, **260**, 87.
- ¹⁰ M Becucci, NM Lakin, G Pietraperzia, E Castellucci, P Brechnac, *J. Chem. Phys.*, 1999, **110**, 9961.
- ¹¹ I López-Tocón, JC Otero, M Becucci, G Pietraperzia, and E Castellucci, *Chem. Phys.*, 1999, **249**, 113.
- ¹² P. Hobza, O. Bludský, H. L. Selzle and E. W. Schlag, *J. Chem. Phys.*, 1992, **97**, 335.
- ¹³ P. Hobza, H. L. Selzle and E. W.; Schlag, *Chem. Rev.*, 1994, **94**, 1767.
- ¹⁴ J. Vacek and P. Hobza, *J. Phys. Chem.*, 1995, **99**, 17088.
- ¹⁵ J. Vacek and P. Hobza, *Int. J. Quant. Chem.*, 1996, **57**, 551.
- ¹⁶ J. Vacek, P. Hobza and J. Jortner, *J. Phys. Chem. A*, 1998, **102**, 8267.
- ¹⁷ J. Cerny, X Tong, P. Hobza, K. Muller-Dethlefs, *J. Chem. Phys.*, 2008, **128**, 114319.
- ¹⁸ M. Biczysko, G. Piani, M. Pasquini, N. Schiccheri, G. Pietraperzia, M. Becucci, M. Pavone and V. Barone, *J. Chem. Phys.*, 2007, **127**, 144303.
- ¹⁹ M. Pasquini, N. Schiccheri, G. Piani, G. Pietraperzia, M. Becucci, M. Biczysko, M. Pavone and V. Barone, *J. Phys. Chem. A*, 2007, **111**, 12363.
- ²⁰ G. Pietraperzia, M. Pasquini, F. Mazzoni, G. Piani, M. Becucci, M. Biczysko, D. Michalski, J. Bloino and V. Barone, *J. Phys. Chem. A*, 2011, **115**, 9603.

- ²¹ C. G. Eisenhardt, M. Pasquini, G. Pietraperzia and M. Becucci, *Phys. Chem. Chem. Phys.*, 2002, **4**, 5590.
- ²² M. S. Bowen, M. Becucci, R. E. Continetti, *J. Phys. Chem. A*, 2005, **109**, 11781.
- ²³ F. Michels, F. Mazzoni, M. Becucci and K. Müller-Dethlefs, to be subm. to *Chem. Phys. Lett.*
- ²⁴ H.-J. Dietrich, R. Lindner and K. Müller-Dethlefs, *J. Chem. Phys.*, 1994, **101**, 3399.
- ²⁵ R. Lindner, H.-J. Dietrich and K. Müller-Dethlefs, *Chem. Phys. Lett.*, 1994, **228**, 417.
- ²⁶ S. Grimme, J. Antony, S. Ehrlich and H. Krieg, *J. Chem. Phys.*, 2010, **132**, 154104.
- ²⁷ S. Grimme, S. Ehrlich and L. Goerigk, *J. Comp. Chem.*, 2011, **32**, 1456.
- ²⁸ F. Weigend, R.; Ahlrichs, *Phys. Chem. Chem. Phys.*, 2005, **7**, 3297.
- ²⁹ A. D. Becke, E. R. Johnson, *J. Chem Phys.*, 2005, **122**, 154101.
- ³⁰ E. R. Johnson, A. D. Becke, *J. Chem. Phys.*, 2005, **123**, 024101.
- ³¹ E. R. Johnson, A. D. Becke, *J. Chem. Phys.*, 2006, **124**, 174104.
- ³² L. Goerigk, H. Kruse, S. Grimme, *Chem. Phys. Chem.*, 2011, **12**, 3421.
- ³³ R. Ahlrichs, M. K. Armbruster, R. A. Bachorz, M. Bär, H.-P. Baron, R. Bauernschmitt, F. A. Bischoff, S. Böcker, N. Crawford, P. Deglmann, F. D. Sala, M. Diedenhofen, M. Ehrig, K. Eichkorn, S. Elliott, F. Furche, A. Glöß, F. Haase, M. Häser, C. Hättig, A. Hellweg, S. Höfener, H. Horn, C. Huber, U. Huniar, M. Kattannek, W. Klopper, A. Köhn, C. Kölmel, M. Kollwitz, K. May, P. Nava, C. Ochsenfeld, H. Öhm, M. Pabst, H. Patzelt, D. Rappoport, O. Rubner, A. Schäfer, U. Schneider, M. Sierka, D. P. Tew, O. Treutler, B. Unterreiner, M. von Arnim, F. Weigend, P. Weis, H. Weiss, N. Winter, *TURBOMOLE 6.5; Universität Karlsruhe, 2009. Available at: <http://www.turbomole.com>.*
- ³⁴ S. Tsuzuki, K. Honda, T. Uchimaru, M. Mikami, K. Tanabe, *J. Am. Chem. Soc.*, 2002, **124**, 104.

- ³⁵ S. Boys, F. Bernardi, *Mol. Phys.*, 1970, **19**, 553.
- ³⁶ T. Helgaker, W. Klopper, H. Koch and J. Noga, *J. Chem. Phys.*, 1997, **106**, 9639.
- ³⁷ D. E. Woon and T. H. Dunning, *J. Chem. Phys.*, 1994, **100**, 2975.
- ³⁸ J. Schirmer, *Phys. Rev. A*, 1982, **26**, 2395.
- ³⁹ A. B. Trofimov, J. Schirmer, *J. Phys. B-At. Mol. Opt.*, 1995, **28**, 2299.
- ⁴⁰ C. Hättig, Structure Optimizations for Excited States with Correlated Second-Order Methods: CC2 and ADC(2). In *Advances in Quantum Chemistry, Vol 50: A Tribute to Jan Lindenberg and Poul Jorgensen*; Sabin, J. R., Brandas, E., Eds., 2005, Vol. 50; pp 37-60.
- ⁴¹ F. Weigend, M. Häser, H. Patzelt and R. Ahlrichs, *Chem. Phys. Lett.*, 1998, **294**, 143.
- ⁴² C. Hättig, *Phys. Chem. Chem. Phys.*, 2005, **7**, 59.
- ⁴³ A. N. Kocharian, G. W. Fernando, K. Palandage, and J. W. Davenport, *Phys. Rev. B*, 2008, **78**, 075431.
- ⁴⁴ A. N. Kocharian, G. W. Fernando, K. Palandage, and J. W. Davenport, *Phys. Rev. B*, 2006, **74**, 024511.
- ⁴⁵ M. Becucci, G. Pietraperzia, N. M. Lakin, E. Castellucci, P. Bréchnac, *Chem. Phys. Lett.*, 1996, **260**, 87.
- ⁴⁶ M. Pradhan, C. Li, J. L. Lin, W. B. Tzeng, *Chem. Phys. Lett.*, 2005, **407**, 100.